29th AIAA Applied Aerodynamics Conference
27 - 30 June 2011, Honolulu, Hawaii

AIAA 2011-3806

Wind Turbine Optimization Under Uncertainty with High Performance Computing

Giovanni Petrone* and Carlo de Nicola †
University of Naples "Federico II", Napoli, 80120, Italy.

Domenico Quagliarella‡
Centro Italiano Ricerche Aerospaziali (CIRA), Capua, 81043, Italy.

Jeroen Witteveen§ , John Axerio-Cilies¶ and Gianluca Iaccarino‖
Mechanical Engineering Departement, Stanford University, Stanford, CA, 94305, USA.

The widespread proliferation of wind turbines for power generation is driving the development of devices that are both efficient and minimally disruptive to surrounding communities. Optimized configurations can become ineffective in the presence of unexpected operating scenarios, for example in the presence of insect or dust contamination, thus requiring recalibration and adjustments. Robust design procedures aim at limiting the potential impact of uncertainties on performance and are an effective risk-mitigation strategy. In this work a wind turbine multi-physics simulation tool – *EOLO* – that represents the aerodynamic loading, realistic turbulent wind scenarios, fluid-structural interactions and acoustics is presented. The geometrical configuration of a realistic turbine is optimized under insect contamination (input uncertainty) using a novel Simplex Stochastic Collocation (SSC) method. This methodology provides a wealth of information regarding the overall performance statistics (output uncertainties) and forms the basis for the exploration of several robust design options. We introduce a new process that extends the usual concept of variance minimization. The proposed robust design strategy is coupled to a customized multi-objective genetic algorithm. The overall process requires a large number of computations and therefore we developed a simulation environment– *LELAND* –to carry out these analysis on large scale parallel clusters. Leland is a dynamic scheduler that starting from a small initial set of computations automatically selects the new candidate simulations to be performed to increase the efficiency of both the optimization procedure and the uncertainty quantification method.

I. Introduction and motivations

Wind turbine design continues to receive considerable attention due to the desire to increase energy production while limiting the environmental impact. Large scale horizontal turbines have benefitted considerably from the use of simulation tools and computational optimization;[1] analysis ranging from the geometrical design of turbine sections[2] to control strategies to maximize the energy capture[3] have appeared in the literature, among many other works.

Most applications of optimization typically ignore the presence of uncertainties in both the environmental conditions, the blade geometry and structural properties. Rigorous quantification of the impact of such uncertainties can fundamentally improve the state-of-the-art in computational predictions and, as a result, provide aid in the design of more cost-effective devices. In this work we focus on geometrical perturbations

*Ph.D. Candidate, Department of Aerospace Engineering, P.le Tecchio 80, 80120 Napoli, Italy.
†Professor, Department of Aerospace Engineering, P.le Tecchio 80, 80120 Napoli, Italy.
‡Senior Researcher, Department of Applied Aerodynamic and Aeroacoustics, Via Maiorise, 81043 Capua, Italy.
§Postdoctoral Fellow, Center for Turbulence Research, Stanford, CA, 94305, USA.
¶Ph.D. Candidate, Mechanical Engineering Department, Stanford, CA, 94305, USA.
‖Assistant Professor, Mechanical Engineering Department, Stanford, CA, 94305, USA.

induced by dust or insect contamination, although the methodology used can be extended without modifications to the other types of uncertainties.[6] We represent the uncertainty as purely stochastic, i.e. a measure of variability and our goal is to establish quantitatively its effect on multiple metrics, namely the power coefficient and the overall noise level. The computational procedure is obviously modified by the presence of uncertainty, but more importantly we explore novel approaches to reformulate the optimization process in this context. One of the important contributions of this paper is the introduction of a novel optimization concept based on the overall probabilistic description of the turbine performance under uncertainty, instead of limiting the analysis to a characterization of the low-order statistical moments (expected performance and its variance).[4]

The present multi-phsycs computational framework constructed around tools developed mainly at the National Renewable Energy Laboratory (NREL). These tools are essentially *deterministic*: once the wind-turbine configuration and other input conditions are specified, the solution is uniquely determined. On the other hand, when uncertainties are present, the results are expressed statistically, e.g. as random variables. The computations become *probabilistic* in nature and it is necessary to propagate the input variability into the output of interest. The approach we follow here is strictly non-intrusive, in the sense that the existing tools are used without modifications, but the solution - or more precisely, its probability distribution - is constructed performing an ensemble of deterministic analyses. The input uncertainty is derived from insect contamination data available in the literature and its main effect is to impact the location of the transition from laminar to turbulent flow over the turbine blade. The optimization process is based on a parametrization of the blade cross-sections and is based on a genetic algorithm.

The paper is organized as followed. The computational framework developed and tested in the present work is illustrated in Section II. Additionally, the cost increase of multiple multi-physics simulations justifies the adoption of a meta-scheduler like *Leland*, presented in section V. In Section III we describe the Simplex Stochastic Collocation (SSC) method as a suitable choice to couple with the optimization process described in Section IV. In Section VI we gather information from literature regarding insect contamination and show in Section VII its impact on both aerodynamic performance and noise and show in Section VIII the overall effect on the optimization process.

II. `EOLO`: a multi-physics low-order model for wind turbines

Wind turbines are multi-physics devices in which the aerodynamic performance, the structural integrity of the blades, the energy conversion toolbox and the acoustic impact have to be carefully examined to achieve an effective design. Each one of these factors introduces considerable complexity if detailed simulations are needed. The aerodynamic performance is dominated by the design of the blade cross-sections. The sections are typically laminar flow airfoils use to reduce the overall drag. The flow characterization is complicated by the need to predict laminar/turbulent transition under a variety of clean and perturbed wind conditions, the inherent angle of attack variability associated with rotation, the presence of dynamic stall, aeroelasticity, etc. In spite of the development of advanced computational fluid dynamic tools that can predict with reasonable accuracy the aerodynamic performance of rotors,[5] the computations remain extremely expensive and often rely on simple models to capture important effects, such as transition, and are generally not considered to be predictive for extreme events such as stall. In this work, we focus on building a flexible computational infrastructure based on low-fidelity models that are connected together in a *matlab* environment `EOLO`.[6] There are two main advantages resulting from this choice: *i)* control and flexibility in using different models developed for capturing complex phenomena, *ii)* low computational cost. It is the second advantage that fundamentally enables us to perform analysis under uncertainty. The flow-chart of the simulation tools is described in details in our previous work.[6] The performance metrics used in the following analysis are the power coefficient and the overall noise level. Representative results corresponding to these two metrics are reported in Fig. 1.

III. Uncertainty analysis

The simulation environment described above can be used effectively to study wind turbine performance in the absence of uncertainties. As mentioned earlier we limit our analysis to uncertainties that can be described using random variables (aleatory uncertainties) and, therefore, our goal is to construct a probabilistic framework around the `EOLO` environment. The most straightforward choice is to perform Monte Carlo (MC)

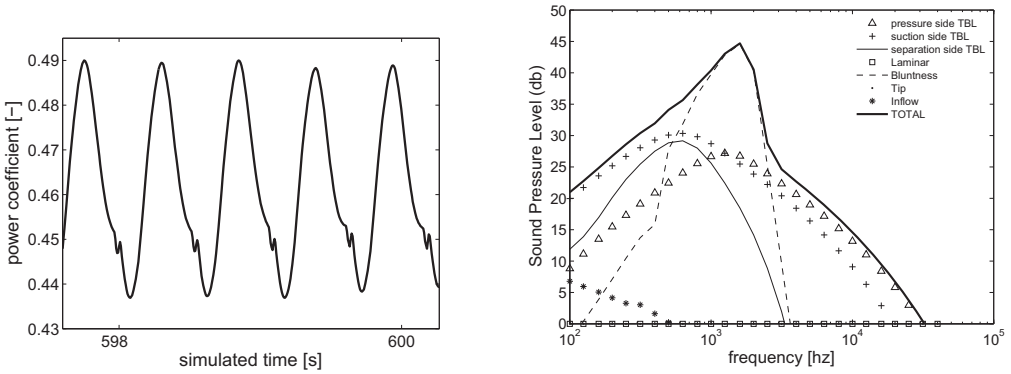

(a) Characteristic cycles of power coefficient

(b) Breakdown of the noise for a microphone located at (x,y,z)=(-20m,0m,0m)

Figure 1. Metrics of interest in the design under uncertainty.

sampling in which many deterministic simulations corresponding to randomly chosen input conditions are performed and a statistical characterization is obtained directly from this ensemble. It is well known that typically a very large ensemble is required to achieve convergence of the statistics of the quantities of interest. We introduce an alternative approach that allows us to obtain equivalent results using a limited number of `EOLO` simulations. In the following we generally refer to the input uncertain variables as ξ and refer to the *space* spanned by these variables as the *parameter* (or probability) space to distinguish it from the physical variable space.

The method used in this work is the Simplex Stochastic Collocation (SSC) approach and it is described in detail in previous works.[7,8] Here we only provides a brief description. SSC uses an initial number of solutions (sampling points) corresponding to different random evaluations of the input parameters and builds a set of non-overlapping simplex elements using a Delaunay triangulation. In each simplex, a response surface of the quantity of interest is built using a polynomial reconstruction. Higher order polynomials are used if the surface is smooth and criteria mutuated from extreme diminishing principles are used to ensure the absence of overshoots.[7]

The initial samples are located at the extrema of the parameter range and at the nominal conditions, see Figure 2a for a two-dimensional example. The discretization is adaptively refined by calculating a refinement measure that combines curvature information and probability mass in each of the simplexes.

A new sampling point is then added randomly in the simplex with the highest measure and the Delaunay triangulation is updated. The sample is confined to a sub-domain of the simplex to ensure a good spread of the sampling points, see Figure 2a. The refinement to $n_s = 17$ samples, shown in Figure 2, leads to a super-linear convergence by increasing the overall polynomial degree of the reconstructions.

The refinement procedure is parallelized by refining a number of simplexes with the highest refinement measure simultaneously. The sampling procedure is stopped when a global error estimate achieves a sufficiently low tolerance; this estimate is based on the concept of hierarchical surplus.[7]

(a) Refinement of the initial mesh

(b) Refined mesh for 17 samples

Figure 2. Simplex Stochastic Collocation discretization of a two–dimensional probability space.

In the wind turbine simulations and other large-scale problems, it is possible that one of the deterministic computations for a specific sample of the random parameters does not converge or gives an unrealistic result. This situation creates no problem to the SSC because of the flexibility of the randomized refinement sampling. The *failed* computation is automatically replaces with another randomly selected point in the simplex element to be refined. If the failed sample is located in the initial discretization at one of the parameter range extrema, an extrapolation is used to extend the reconstructed surfaces from the other simplexes. In the analysis performed in this paper, this has proven to be an effective approach for dealing with erroneous samples.

IV. Optimization strategy

IV.A. Genetic Algorithms

The optimization strategy is based on well-known Genetic Algorithms[35] (or GAs). A GA consists of i) a finite population of individuals of an assigned size - each of them usually encoded as a string of bits named genotype, ii) an adaptive function, called fitness - this provides a measure of the individual to adapt to the environment, an estimate of the quality of the solution, and an indication on the individuals most likely to reproduce, and iii) semi-random genetic operators such as selection crossover and mutation - these operate on the genotype expression of individuals, changing their associated fitness.

In general, the GA optimization process requires the definition of a potentially large number of candidate design and the evaluation of the corresponding solutions. Successive generation of candidate design are considered until no further improvement is obtained. From a computational point of view both the uncertainty quantification and the optimization procedures require the management of large ensemble of nearly identical simulation. In the next section we describe an efficient computational framework to handle these ensemble; in the following subsections we describe in details the optimization problem and the concept of robustness.

IV.B. Definition of the shape optimization problem

We follow Zhong and Qiao's work[36] and use B-splines to parameterize the geometry. Specifically, we consider fifth order B-splines with a nominal uniform knot set to represent both the cross-sections of the turbine blades and the distribution of the chord and twist along the span. The geometry of the base airfoils is given by the following equations

$$f = f_0 + \sum_{1}^{n_f} P_i N_i(X) \tag{1}$$

$$g = g_0 + \sum_{n_f+1}^{n_f+n_g} P_i N_i(X) \tag{2}$$

where f and g are the upper and bottom surface, f_0 and g_0 are the initial bottom and upper surface, P_i are the control points of the B-splines and $N_i(X)$ are the B-spline basis functions. Three geometrical constraints are enforced: the first is to avoid intersections of the upper and lower airfoil surfaces, the second is to reduce the changes in curvature in either the upper or lower surface of the airfoil, and the third is for to enforce a maximum thickness of the airfoils.

The chord and twist distributions are also parametrized similarly using B-splines:

$$\theta = \theta_0 + \sum_{1}^{n_\theta} P_i N_i(X) \tag{3}$$

$$chord = chord_0 + \sum_{1}^{n_{chord}} P_i N_i(X) \tag{4}$$

where θ and $chord$ are the distribution of twist and chords after optimization, θ_0 and $chord_0$ are the initial distribution of twist and chords, P_i are the control points of the B-splines and $N_i(X)$ are the B-spline basis functions. The degree of the B-splines chosen for twist and chord optimization is three. It should be noted that when all the control points of the airfoil parametrization and of the chord and twist distribution have zero values the original shape is returned.

The optimization process (in the absence of uncertainties) uses an in-house non-dominated sorting GA (NSGA) algorithm that considers as objectives the maximization of the averaged power coefficient over the last minute of the simulation [-] and the minimization of the Overall Sound Pressure Level [dB] at the observer location.

IV.C. Robust Optimization

The concept of robust optimization is intuitively connected to the idea that in the presence of (input) uncertainty the optimal design should be relatively insensitive (small output uncertainty). We will review three commonly used robustness principle before introducing a novel, and more general, definition. The three strategies can be simply considered as variants of constraint and non-constraint optimization and an extension of multiobjective optimization.

Let's consider an objective function in the form $f(z,\xi)$ where $z \in Z$ represents a design variable and $\xi \in \Omega$ represents the input uncertainty (which can be either a design variable or another parameter in the problem). A minimization problem is formulated in general as: find $\overline{z} \in Z$ such that

$$f(\overline{z},\xi) \leq f(z,\xi) \quad \forall z \in Z, \ \forall \xi \in \Omega \tag{5}$$

A robust design is defined as one whose performance remains relatively unchanged (and feasible) in the presence of uncertainty. In a probabilistic framework for uncertainty analysis (such as the one introduced earlier) the problem is that $f(z,\xi)$ is a random quantity induced by ξ. It is possible to introduce an operator Φ, applied to $f(z,\xi)$ in order to obtain a real-valued attribute of it, reducing the problem to finding $\overline{z} \in Z$ such that

$$\Phi(f(\overline{z},\xi)) \leq \Phi(f(z,\xi)) \quad \forall z \in Z \tag{6}$$

Different definition for Φ might be used, for example $\Phi(f(z,\xi))$ are the statistical moments of f. The simplest choice is obviously the expected value of f: (referred to as **Bayes Principle**[37]):

$$\Phi\left(f(z,\xi)\right) = \int_{\Omega} f(z,\xi)\Psi_{\xi} d\xi = \mu(z) \tag{7}$$

where Ψ_{ξ} is the probability density function of ξ. Other (higher order) moments can be used (**Mean Value Penalty Optimization**):

$$\Phi\left(f(z,\xi)\right) = w_1\mu(z) + \left(\sum_{k=2}^{N} w_k m^k\left(f(z,\xi)\right)\right)^{1/2} \tag{8}$$

where $w_1, ..., w_N$ are (tunable) weights, N is the maximum order of statistical moments considered and $m^k\left(f(z,\xi)\right)$ is the k-th order moment of $f(z,\xi)$

$$m^k\left(f(z,\xi)\right) = \int_{\Omega} \left(f(z,\xi) - \mu(z)\right)^k \Psi_{\xi} d\xi \tag{9}$$

which leads to (for $w_1 = w_2 = 1$ and $N = 2$)

$$\Phi\left(f(z,\xi)\right) = \mu(z) + \sigma(z) \tag{10}$$

where $\sigma^2(z)$ is the variance of $f(z,\xi)$. In this case the optimization under uncertainty seeks to minimize the mean plus standard deviation, giving a formal and mathematically sound construction for the idea of insensitive design.

Another approach, interpreted as a **Constrained Optimization**, can be formulated in finding $\overline{z} \in Z$ such that

$$\begin{cases} \mu(\overline{z}) \leq \mu(z) \quad \forall z \in Z \\ \text{s.to:} \qquad\qquad m^k\left(f(z,\xi)\right) \leq C_k \ \forall k \in 2, N \end{cases} \tag{11}$$

where C_k is a constraint on the the order k central moment of $f(z,\xi)$. Again for N=2 this procedure reduces in finding $\overline{z} \in Z$ such that

$$\begin{cases} \mu(\overline{z}) \leq \mu(z) \quad \forall z \in Z \\ \text{s.to:} \qquad\qquad \sigma^2(z) \leq \sigma^* \end{cases} \tag{12}$$

where σ^* is the maximum value allowed for the variance.

Finally, a fourth approach formulates the problem as a **Multi-objective Approach** in the form

$$\begin{cases} \min\limits_{Z} \mu(z) \\ \min\limits_{Z} m^k \left(f(z,\xi)\right) \ \forall k \in 2, N \end{cases} \tag{13}$$

which for N=2 becomes

$$\begin{cases} \min\limits_{Z} \mu(z) \\ \min\limits_{Z} \sigma^2 \left(z\right) \end{cases} \tag{14}$$

IV.D. A novel CDF based approach

In the previous approaches the objective function is transformed into a different form in order to eliminate its random character (reduce the dependency on ξ). One of the consequences is that typically only the mean and the variance of the objective function are considered in the process, thus potentially eliminating important characteristics of its probabilistic description (only for a Gaussian random variable the mean and the variance completely describe the overall distribution). The goal of the approach proposed here is to i) avoid any assumptions on the type of the objective function i.e. Gaussianity and ii) avoid increasing the dimensionality of problem (as in the multiobjective robust optimization). Let us assume a reference solution, namely the RAO (Reference Absolute Optimum), which we define as the inferior limit of the objective function in the presence of uncertainties and which corresponds to an ideal deterministic optimum

$$RAO = \inf_{Z \times \Omega} f(z,\xi) \tag{15}$$

The ideal solution of a problem of optimization under uncertainty is a design that ensures the lowest possible value of the objective function (the RAO) with no sensitivity on the uncertain quantities.

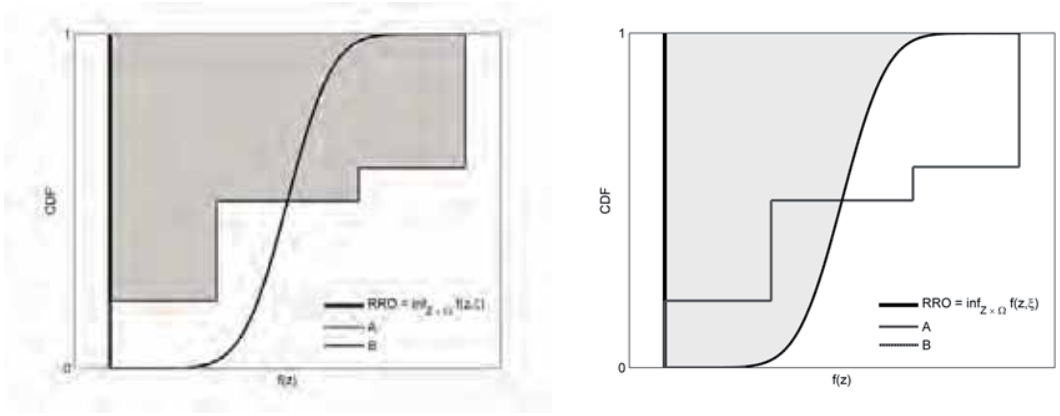

(a) The shaded area is the RI for candidate design A (b) The shaded area is the RI for candidate design B

Figure 3. CDF based measure of robustness

In terms of the Cumulative Density Function (CDF) the RAO is represented by a vertical line and assumed to be a reference for the proposed method. Every actual design, being subject to uncertainty, will be represented by a distribution with a non-zero support. The main concept we introduce is to identify a measure of the difference between the CDFs of the RAO and any other design to direct the optimization process. Many possible measures of distance between distributions can be considered; here we use the area metric,[51] also referred to as the Minkowski L_1 metric; the area between the CDF of the RAO and the CDF of the candidate design, F(z), is the measure of the mismatch between them and gives information about the robustness of the candidate design (RI - Robustness Index).

$$RI(z) = \int_{-\inf}^{\inf} |F(z) - \delta_z(RAO)| \, d\xi \tag{16}$$

where δ_z is the Dirac delta function. The RI generalizes the deterministic comparison of scalar values that have no uncertainty or the difference between statistical moments (as used in many robust optimization algortihms); if the candidate design is deterministic, the CDF is a Dirac function centered on one value (like it is for RAO or any scalar point values) and in this case the area is equal to the difference between two scalar values. The RI will tend not to be overly sensitive to minor discrepancies in the distribution tails (assuming the area is finite), because it reflects the full distribution of the scalar point values. In particular, it is clearly not merely a measure of the difference in the means and/or variances, but takes into account the overall difference between distributions. Another useful property of this measure, is that its units are are identical to the objective function units. This property is useful in i) the ranking process (as shown in the next section) and to ii) make the measure is intuitively meaningful. Using the concept of area measure, the robust optimum can be formulated to finding $\overline{z} \in Z$ such that

$$RI(\overline{z}) \leq RI(z) \quad \forall z \in Z \tag{17}$$

which for RI(z)=0 returns the ideal design corresponding to the RAO.

IV.E. Probabilistic rank

The definition of the RI introduced above can be also adopted to construct the optimization algorithm, specifically in the context of multi-obejctive GA, we can extend the concept of ranking by introducing the area metric. For each generation we assume the reference solution to be the one that dominates all others (i.e. rank equal to 1) and assume its CDF to be deterministic, as for the ROA. We define the probabilistic rank as

$$rank_P(z) = 1 + RI(z) \tag{18}$$

The population of solutions corresponding to each generation is sorted using $rank_P(z)$ (as a first criterion), obtaining a non integer value for the rank. This introduces additional information related to the uncertainty in the GA.

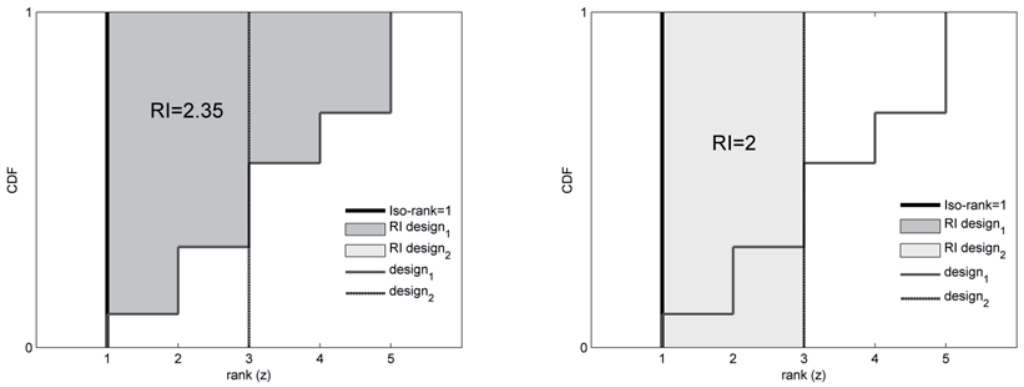

(a) The $rank_P$ for candidate design 1 is 3.35

(b) The $rank_P$ for candidate design 2 is 3

Figure 4. Probabilistic rank

IV.F. Probabilistic non-domination sorting

The original NSGA-II algorithm[50] constructs the sorting procedure of the candidate designs using the rank and the crowding distance operators. The aim of the proposed procedure is to obtain an algorithm which generalizes these operators. As a direct consequence of the introduction of the probabilistic rank, we can assume all the designs falling between two contiguous integer values of the probabilistic rank to have a similar probabilistic domination in the Pareto sense (i.e the original discrete layers of dominations become continuous). In each continuous "layer" we can use in sequence i) the non-integer part of the rank and ii) a mean measure of the crowding distance to distinguish among designs - we can cluster points where the RI is lower (enhanced probabilistic domination) while preserving density and coverage. In the case of a population

of deterministic candidate designs, the probabilistic rank reduces to the its deterministic counterpart (i.e. integer) and the mean crowding distance reduces to the crowding distance.

IV.G. Analytic test case

In this subsection we compare the results obtained with the Bayes Principle and the Mean Value penalized by the standard deviation, with the proposed probabilistic sorting on the following multi-objective test case

$$f_1(z,\xi) = (y_1(z,\xi) - 1)^2 + (y_1(z,\xi) - y_2(z,\xi))^2 \tag{19}$$
$$f_2(z,\xi) = (y_2(z,\xi) - 3)^2 + (y_1(z,\xi) - y_2(z,\xi))^2 \tag{20}$$

where

$$y_1(z,\xi) = \xi_1 + \xi_3 \times z_1 \tag{21}$$
$$y_2(z,\xi) = \xi_2 + \xi_4 \times z_2 \tag{22}$$

The characteristics of the design variables and uncertainties are listed in Table 1.

Table 1. Analytic test case: design variables and uncertainties

Label	Type	Distribution	Range
z_1	design variable		$[-5, 5]$
z_2	design variable		$[-5, 5]$
ξ_1	uncertain variable	uniform	$[-0.3, 0.2]$
ξ_2	uncertain variable	uniform	$[-0.2, 0.3]$
ξ_3	uncertain variable	uniform	$[-0.9, 1.2]$
ξ_4	uncertain variable	uniform	$[-0.8, 1.1]$

The mean value and the mean value penalized by the standard deviation condense all the information of the objective function probability distributions into a single value; further statistical details are not used in the optimization process. The Pareto front corresponding to the analytic test function are similar in shape to their deterministic equivalent and no further information about the best design can be extracted from the front as shown in Figure 5.a.

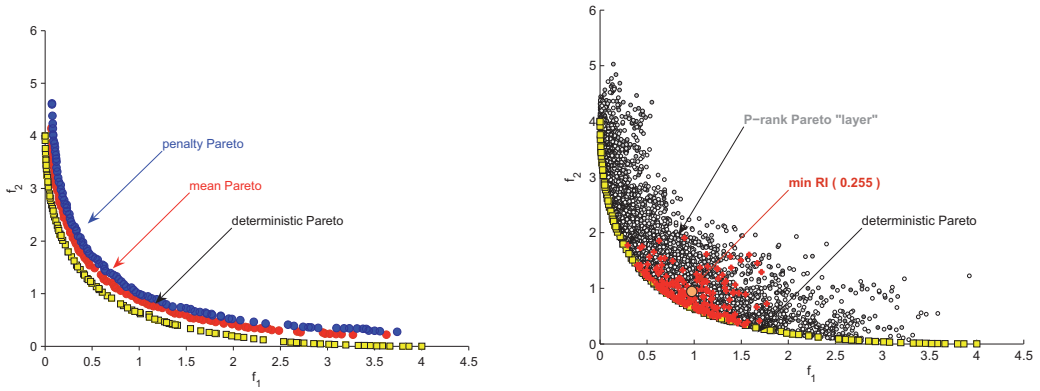

(a) Pareto front corresponding to deterministic scenarios and obtained using mean value and mean value penalized optimization

(b) Pareto front using probabilistic sorting

Figure 5. Analytic test case

The Pareto front constructed using the probabilistic sorting approach consists of a family of clouds (i.e. each cloud represents an uncertain design) characterized by different RI values. The proposed method allows us to take into account the overall probability distribution and provides an additional criterion to distinguish

designs on the same layer. In this test case, the red distribution in Figure 5.b represents the lowest RI value and the corresponding design can be assumed to be the best probabilistic compromise for this optimization problem. It is extremely clear that the distributions are not Gaussians, hence the mean and the variance do not sufficiently represent the stochastic behavior of the objective function.

V. A parallel computational framework for robust optimization: `Leland`

Both the uncertainty quantification methodology and the optimization strategy adopted in this work require the construction of an ensemble of computations. Due to the high cost of each solution - as it is common in multi-disciplinary frameworks (i.e. aerodynamics, structure, control, etc.) - we have developed an environment (hereafter called Leland) for optimal resource allocation on a UNIX multiprocessor cluster. Its structure is based on a workflow managed via matlab through I/O that explicitly connects the software tools involved in the process. Leland is designed to run natively on any high-performance computing (HPC) system, by integrating with the job-submission/queuing system (for example Torque). In Leland a "job" is an instance of the entire multiphysics simulation, which might include grid generation, morphing, flow solution and fluid/structure coupling, acoustic analysis and postprocessing. The main objective of Leland is to set-up a candidate design as a job and to manage it until it is completed in order to gather relevant results that are used to inform the robust optimization process. The various components of Leland are introduced below.

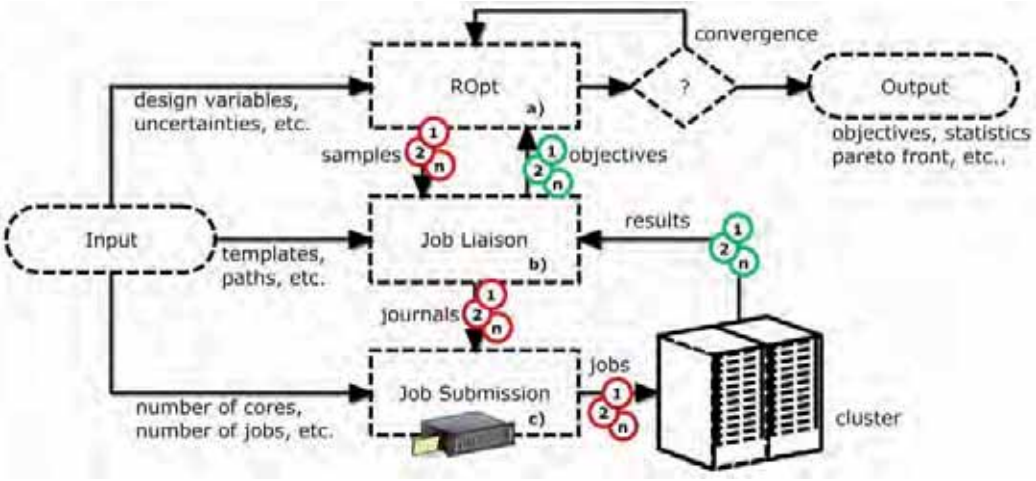

Figure 6. LELAND flowchart

ROpt (robust optimization), shown in figure 6.a, is the engine behind this design environment. Given the design and/or uncertain input variables, ROpt continuously generates new design proposals (samples) based on the evolutionary strategy and/or analysis of the uncertainty space, until a convergence criterion is met. The Job Liaison, shown in figure 6.b, defines the characteristics of each single job and continuously monitors the progress of the simulations until completion in order to communicate the objective evaluations back to ROpt. The Job Submission engine, shown in figure 6.c, ensures that the correct number of jobs are always running on the cluster. The input variables (number of cores, number of jobs, etc.) used to initialize the runs are dynamic, meaning they can be edited on the fly and the system will respond accordingly.

VI. Sources of uncertainty: insect contamination

Several studies on wind turbines[17–20] and fixed wings[21,22] illustrate the effect of insect and dirt contamination on the overall aerodynamic performance. Insects are present in the lower layer of the atmosphere, with a density rapidly decreasing from ground level to 500 ft. Hardy and Milnecite[23] found that the morphology of insects is a function of altitude and that estimation of the actual contamination depends on the operating conditions. In wind-turbines the effect of contamination can be particularly strong when the blade cross-sections are designed to operate in the laminar flow regime. The presence of insect contamination produces boundary layer disturbances that can lead to early turbulence transition with a deterioration in

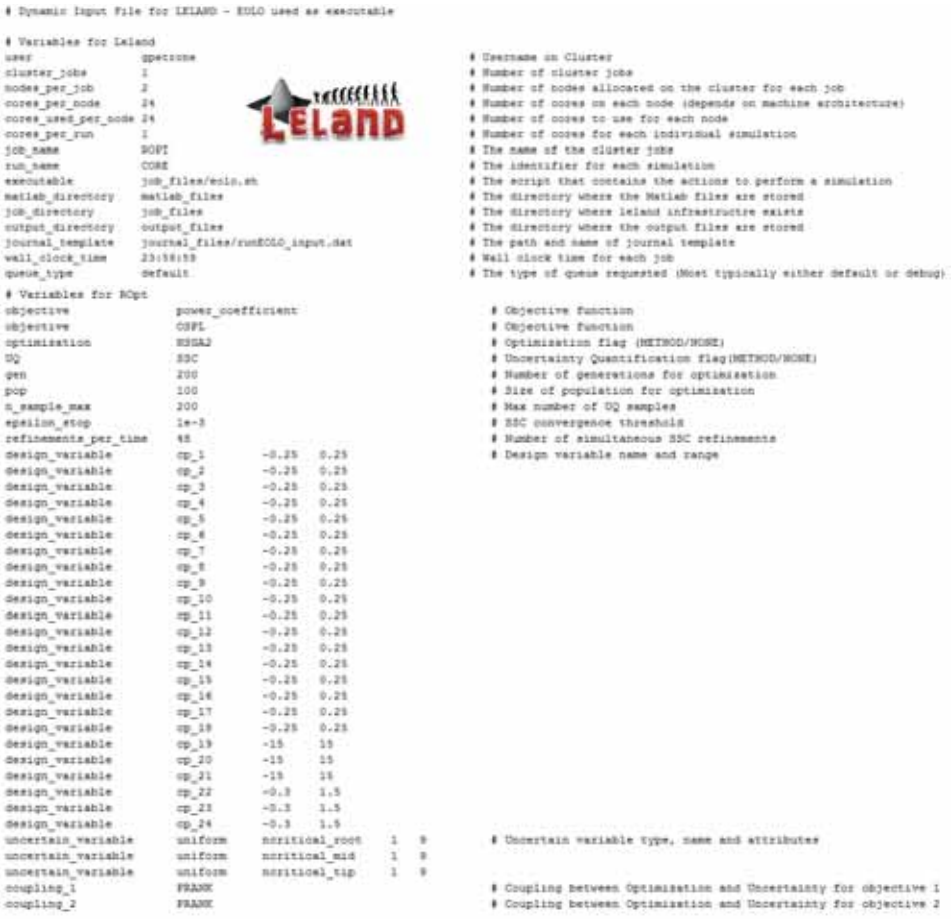

```
# Dynamic Input File for LELAND - EOLO used as executable

# Variables for Leland
user                gpecrone                    # Username on Cluster
cluster_jobs        1                           # Number of cluster jobs
nodes_per_job       2                           # Number of nodes allocated on the cluster for each job
cores_per_node      24                          # Number of cores on each node (depends on machine architecture)
cores_used_per_node 24                          # Number of cores to use for each node
cores_per_run       1                           # Number of cores for each individual simulation
job_name            ROPT                        # The name of the cluster jobs
run_name            CORE                        # The identifier for each simulation
executable          job_files/eolo.sh           # The script that contains the actions to perform a simulation
matlab_directory    matlab_files                # The directory where the Matlab files are stored
job_directory       job_files                   # The directory where leland infrastructre exists
output_directory    output_files                # The directory where the output files are stored
journal_template    journal_files/runEOLO_input.dat # The path and name of journal template
wall_clock_time     23:58:59                    # Wall clock time for each job
queue_type          default                     # The type of queue requested (Most typically either default or debug)

# Variables for ROpt
objective           power_coefficient           # Objective function
objective           COPL                        # Objective function
optimization        NSGA2                       # Optimization flag (METHOD/NONE)
UQ                  SSC                         # Uncertainty Quantification flag(METHOD/NONE)
gen                 200                         # Number of generations for optimization
pop                 100                         # Size of population for optimization
n_sample_max        200                         # Max number of UQ samples
epsilon_stop        1e-3                        # SSC convergence threshold
refinements_per_time 48                         # Number of simultaneous SSC refinements
design_variable     cp_1    -0.25   0.25        # Design variable name and range
design_variable     cp_2    -0.25   0.25
design_variable     cp_3    -0.25   0.25
design_variable     cp_4    -0.25   0.25
design_variable     cp_5    -0.25   0.25
design_variable     cp_6    -0.25   0.25
design_variable     cp_7    -0.25   0.25
design_variable     cp_8    -0.25   0.25
design_variable     cp_9    -0.25   0.25
design_variable     cp_10   -0.25   0.25
design_variable     cp_11   -0.25   0.25
design_variable     cp_12   -0.25   0.25
design_variable     cp_13   -0.25   0.25
design_variable     cp_14   -0.25   0.25
design_variable     cp_15   -0.25   0.25
design_variable     cp_16   -0.25   0.25
design_variable     cp_17   -0.25   0.25
design_variable     cp_18   -0.25   0.25
design_variable     cp_19   -15     15
design_variable     cp_20   -15     15
design_variable     cp_21   -15     15
design_variable     cp_22   -0.3    1.5
design_variable     cp_23   -0.3    1.5
design_variable     cp_24   -0.3    1.5
uncertain_variable  uniform  ncritical_root  1  9   # Uncertain variable type, name and attributes
uncertain_variable  uniform  ncritical_mid   1  9
uncertain_variable  uniform  ncritical_tip   1  9
coupling_1          FRANK                       # Coupling between Optimization and Uncertainty for objective 1
coupling_2          FRANK                       # Coupling between Optimization and Uncertainty for objective 2
```

Figure 7. LELAND input file for EOLO

aerodynamic performance. This is the motivation for including insect contamination as a leading cause of uncertainty in the present analysis of wind turbines.

Crouch *et al*[25] studied the effects of surface protrusions (steps) on the turbulence transition in boundary layers experimentally. They also modified the e^N method to capture the observed transition modifications, via a reduction of the critical N-factor:

$$N_{crit} = N_{crit^0} - \Delta N_{crit}(\frac{h}{\delta^*}) \tag{23}$$

where h is the height of the step (i.e. the accumulated insect height)[m], δ^* is the boundary layer displacement thickness at the step location [m], ΔN_{crit} accounts for the local change in the stability characteristics at the step[-] and N_{crit^0} is the clean value of the critical N-factor[-].

In this work we assume that the insect impact produces roughness that leads to modification of the N-factor. We consider three independent variables describing the N-factor ranging from clean conditions ($N_{crit} = 9$) to transition bypass ($N_{crit} = 1$) at the root, midspan and tip sections of a turbine blade.

VII. Analysis under uncertainty

The AOC 15/50 is a downwind turbine, i.e. its blades rotate downwind of the drive train assembly. Furthermore, it has no active yaw control and depends on its blades to track the wind. This wind turbine is the evolution of the rugged and reliable Enertech E44, many of which were installed in the 1980's and are still running today. Independent analysis and testing at NREL, the Netherlands Energy Research Foundation (ECN), RISO Laboratory in Denmark, the Atlantic Wind Test Site (AWTS) on Prince Edward Island and other sites around the world verify that the AOC 15/50 wind turbine generators are very reliable in

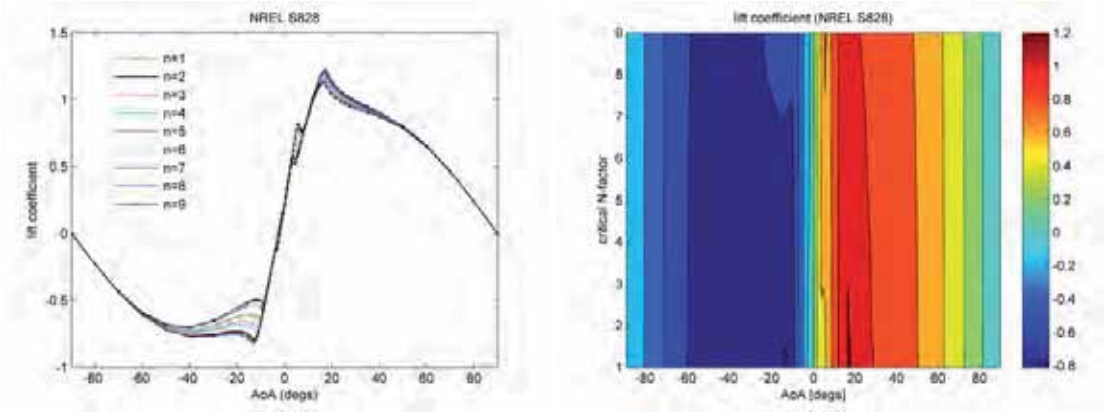

(a) Lift characteristic (b) Contour of lift coefficient

Figure 8. Effect of critical N-factor on NREL S828 cross-section. Re=1015166.4253, M=0.1218.

even the harshest weather conditions. The AOC 15/50 is designed for simplicity to minimize maintenance requirements and to be able to safely operate in normal and extreme conditions. In this section the AOC 15/50 is investigated under uncertainty considering the effect of insect contamination (as described in the previous section). The `EOLO` framework is driven by the SSC routines and the uncertainties directly impact aerodynamic lading computed using `Xfoil`; the present analysis shown an reduction of up to 16% in the averaged power coefficient due to the insect contamination with respect to the clean case. It is worth noting that in the in the literature the effect is even more marked, with up to 50% reduction reported.[17,18] This difference might be due to the present approach used to characterize the effect of the insect contamination.

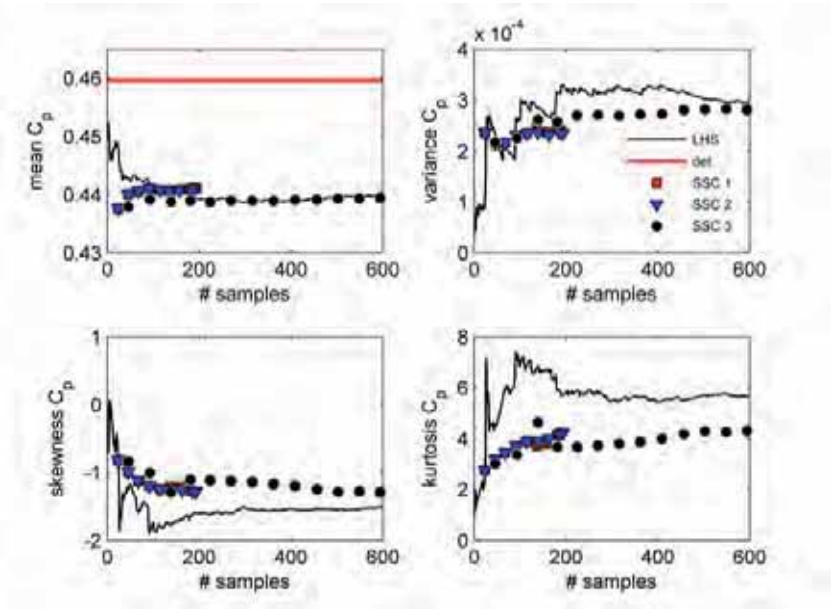

Figure 9. Analysis under uncertainty due to Insect contamination: convergence histories of the mean,variance, skewness and kurtosis of the power coefficient

We compared the predictions using the SSC method with 1000 Monte Carlo realizations illustrating the considerable improvement in the convergence properties of the statistics of the power coefficient (the noise levels also show similar trends). In Fig. 9 we report two SSC computations in which the differences are driven by the randomized adaptive refinement algorithm, to illustrate that the statistics do converge rather quickly.

VIII. Optimization under uncertainty

An initial multi-objective optimization (maximize the power coefficient while minimizing the noise) has been carried out ignoring the insect contamination and the resulting Pareto front is shown in Figure 10. The baseline blade was already optimized by the manufacturer but due to the steep characteristics of the Pareto at high power coefficient it was possible to find a trade-off design with considerable less noise. The population of the GA contained 40 individuals, which evolved for 50 generations.

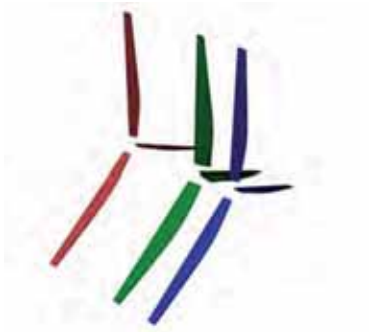

(a) Baseline, Trade-off and higest Performing designs

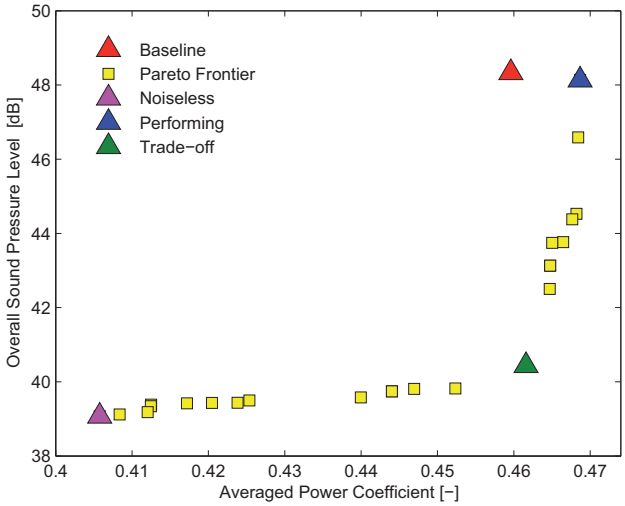

(b) ROpt design

Figure 10. Deterministic Pareto front

Successive simulations were performed accounting for uncertainties due to insect contamination. The deterministic Pareto front was used as initialization for the novel procedure. In Figure 11 a close-up of the design space close to the previous trade-off design is shown. It is important to notice that in the presence of uncertainty each new design is actually stochastic and characterized by a number (cloud) of probable results. This is illustrated in Figure 11.a. A new locus of optimal configurations is extracted (Pareto layer, the first non-dominated layer of Section IV.F): we refer to the trade-off solution in the presence of uncertainty as the ROpt (Robust Optimum) design.

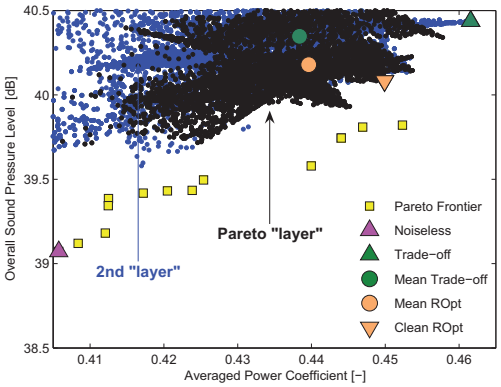

(a) First and second layer of domination

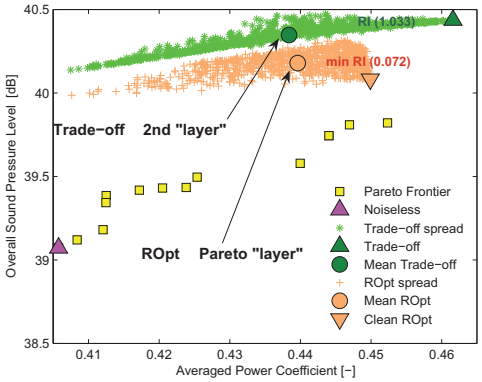

(b) ROpt and Trade-off design

Figure 11. Probabilistic Pareto front [detail]

It is interesting to note that the ROpt design does not lie on the deterministic Pareto front and viceversa,

the deterministic trade-off design does not lie on the probabilistic Pareto layer. Instead, the latter design lies on the second layer and additionally the mean Trade-off configuration is fully dominated by the ROpt design. The RI for the ROpt design assumes the lowest value in the population ($RI = 0.072$) and has been chosen as a decision making criterion for the probabilistic Pareto front, see Figure 11.b. Moreover, the deterministic trade-off design has been chosen as the Best Efficient Point[52] of the deterministic Pareto front.

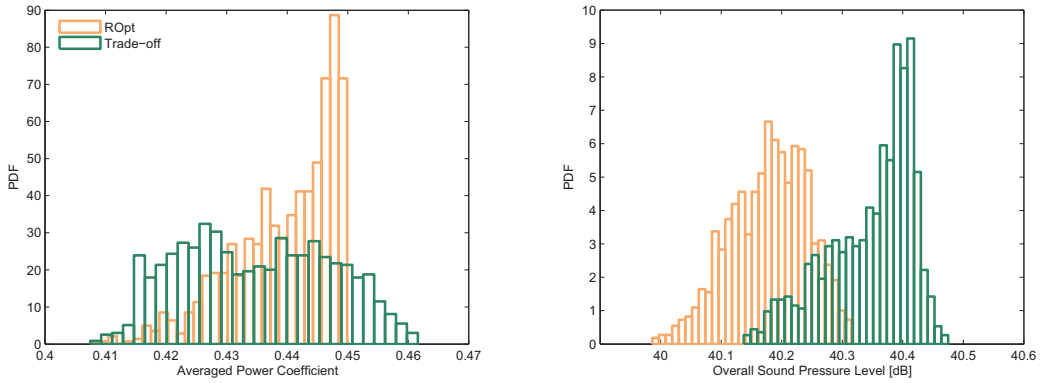

(a) PDF of Averaged Power Coefficient (b) PDF of Overall Sound Pressure Level

Figure 12. Probabilistic and deterministic trade-off designs

The spread of the ROpt designs suggests a stable solution in the presence of uncertainty since it is more probable that a design is located at higher values of the averaged power coefficient and the distribution is rather uniform compared to the trade-off spread, as shown in Figure 12.a. Additionally, the spread of Overall Sound Pressure Level of the ROpt design is clearly dominating the deterministic trade-off, as shown in Figure 12.b. It is interesting to notice that the presented novel method returns as result of the process of robust optimization the optimal design variables and the CDFs of the objective functions: the CDF represents a complete information in probability about the behavior of the candidate design rather than few real value attributes given by the other methods discussed in Section IV.

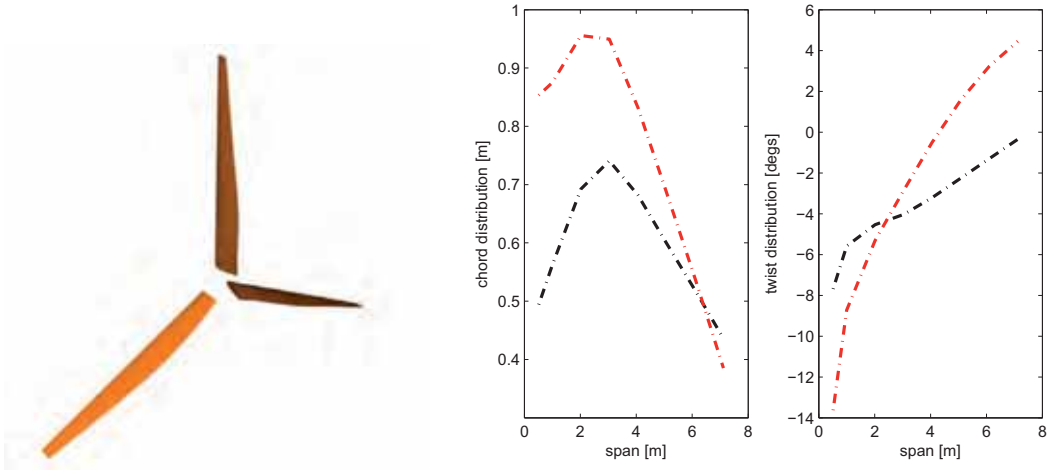

(a) ROpt design (b) ROpt and baseline chord and twist distributions

Figure 13. ROpt design characteristics

The optimized design (red) reveals a significant increase in the length of the chords at the inner part of the blade, while its twist follows a smoother distribution than the baseline (black) showing higher torsion closer to the root and tip sections, as shown in Figure 13.b. The optimized airfoils for the ROpt design are shown in Figure 14 in order to compare them with the baseline solution. It is interesting to notice the

change in the trailing edge at the root section of the blade, which could be related to the noise reduction and the significant change in curvature of the mid-span airfoil. The tip airfoil reveals a significant increase in thickness up to 60% of the chord, with a trailing edge very similar to the baseline solution.

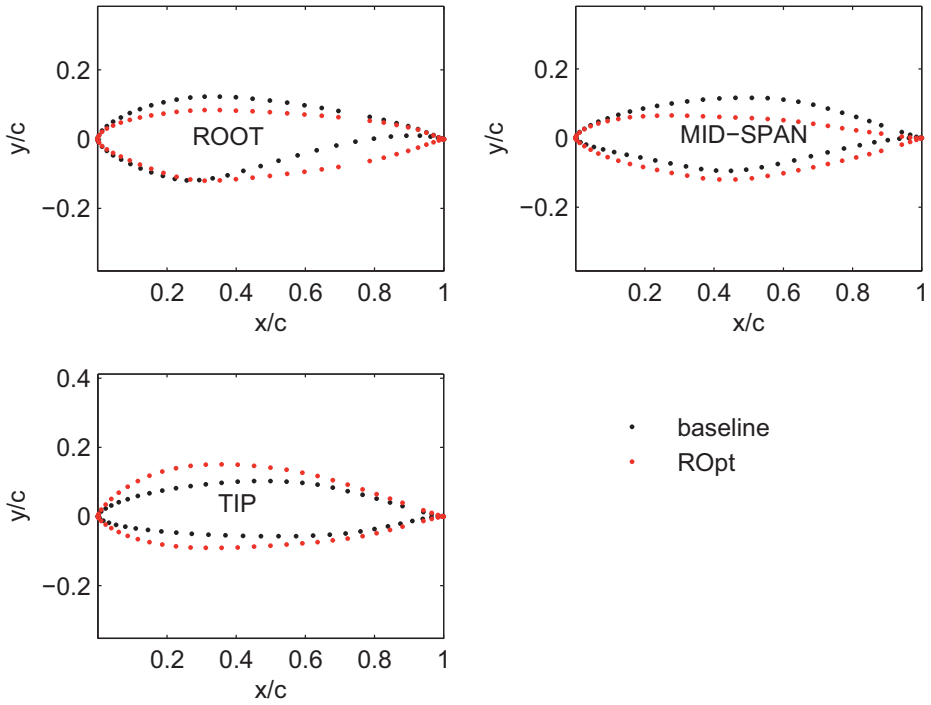

Figure 14. ROpt airfoils

IX. Aknowledgements

Support from the Netherlands Organization for Scientific Research (NWO) under the Rubicon Fellowship program is gratefully acknowledged. GP is supported under the exchange program of the XXIV Doctoral Program in Industrial Engineering (Aeronautics) at the Federico II University in Naples, Italy. The authors are also thankful for additional support from the US DOE program on Uncertainty Quantification under contract DE-FG02-10ER26026 (project manager K. Pao).

X. Conclusions

The present study introduces a novel process of optimization of wind turbine blades under uncertainty. The computations were carried out using a multi-physics model `EOLO` that included aerodynamic predictions, comprehensive structural analysis and acoustic estimation. Moreover, we used a high performance meta-scheduler `Leland` that allowed us to perform a large ensemble of calculations automatically and efficiently on a large cluster. Insect contamination is considered as a source of uncertainty and the present methodology allowed to estimate its effect on aerodynamic performance and noise. We proposed a novel intrusive approach to couple multi-objective optimization and uncertainty quantification in order to let the latter be a driver in the shifting of the Pareto Front due to uncertainties. The proposed approach is based on the full probabilistic description of the objective function under uncertainty and appears promising at overcoming the main drawbacks of other methods found in literature even if further benchmarks are required. The design obtained with the novel procedure appears to be more stable in the presence of uncertainty than its deterministic counterpart, hence the main goal of this work has been successfully achieved.

References

[1]Wang, X., Wen, Z., Wei, J. Z., Sorensen J. Chen, J. Shape optimization of wind turbine blades. Wind Energy Vol. 12 (8), 781–803, 2009.

[2]Kusiak, A., Zhenh, H. Optimization of wind turbine energy and power factor with an evolutionary computation algorithm, Energy Vol. 35, 1324–1332, 2010

[3]Fuglsang P., Bak C. Development of the Riso wind turbine airfoils, Wind Energy Vol. 7 (2), 145–162, 2004.

[4]T. Diveux1, P. Sebastian, D. Bernard, J. R. Puiggali, J. Y. Grandidier Horizontal axis wind turbine systems: optimization using genetic algorithms Wind Energy Vol. 4 (4), 151–171, 2001.

[5]Alonso, J. J., Hahn, S., Ham, F., Herrmann, M., Iaccarino, G., Kalitzin, G., LeGresley, P., Mattsson, K., Medic, G., Moin, P., Pitsch, H., Schluter, J., Svard, M., Van der Weide, E., You, D. and Wu, X., 2006, CHIMPS: A high-performance scalable module for multi physics simulations. AIAA Paper 2006 5274.

[6]Petrone, G., de Nicola, C., Quagliarella, D., Witteveen, J.A.S, Iaccarino, G., Wind turbine performance analysis under uncertainty, 49th AIAA Aerospace Sciences Meeting, Orlando, Florida (2011) AIAA-2011-0544

[7]Witteveen, J.A.S., Iaccarino, G., Simplex Elements Stochastic Collocation for Uncertainty Propagation in Robust Design Optimization 48th AIAA Aerospace Sciences Meeting, Orlando, Florida (2010) AIAA-2010-1313.

[8]Witteveen, J.A.S., Iaccarino, G., Simplex elements stochastic collocation in higher-dimensional probability spaces, 51st AIAA/ASME/ASCE/AHS/ASC Structures, Structural Dynamics, and Materials Conference, Orlando, Florida (2010) AIAA-2010-2924.

[9]Drela, M., Xfoil: An Analysis and Design System for Low Reynolds Number Airfoils, Low Reynolds Number Aerodynamics (Conference Proceedings), edited by T.J. Mueller, University of Notre Dame 1989.

[10]Tangler, J., Kocurek, J.D., Wind Turbine Post-Stall Airfoil Performance Characteristics Guidelines for Blade-Element Momentum Methods, NREL/CP-500-36900.

[11]Tuller, S.E., Brett, A.C., The characteristics of wind velocity that favor the fitting of a Weibull distribution in wind speed analysis. Journal of Climate and Applied Meteorology, 23:124134, 1984.

[12]Antoniou,I., Petersen,S.M., Højstrup,J. et al., Identification of variables for site calibration and power curve assessment in complex terrain. Technical Report JOR3-CT98-0257, Risø, CRES, WindTest, DEWI, ECN, Bonus and NEG Micon, July 2001.

[13]Lange,B., Modelling the Marine Boundary Layer for Offshore Wind Power Utilisation. PhD thesis, University of Oldenburg, December 2002.

[14]Wieringa,J., Rijkoort,P.J., Windklimaat van Nederland (Wind Climate of the Netherlands). KNMI/Staatsuitgeverij, Den Haag, 1983.

[15]Downey,R.P., Uncertainty in wind turbine life equivalent load due to variation of site conditions. Masters thesis, Technical University of Denmark, Fluid Mechanics Section, Lyngby, April 2006.

[16]Veldkamp, D., Chances in Wind Energy - A probabilistic Approach to Wind Turbine Fatigue Design. PhD thesis, Delft University.

[17]Corten G. , Veldkamp H., Insects cause double stall, EWEC Copenhagen , 2001.

[18]Corten, G.P., Insects Cause Double Stall, ECN-CX–00-018, Feb. 2001

[19]Dyrmose, S.Z., Hansen, P., The Double Stall Phenomenon and how to avoid it , IEA, Lyngby, 1998.

[20]Madsen, H.A., Aerodynamics of a Horizontal Axis Wind Turbine in Natural Conditions, Risoe M 2903 1991.

[21]Iachmann, H.S., Aspects of Insect Contamination in Relation to Laminar Flow Aircraft, Aeronautical Research Council current, April 1959.

[22]Croom, C. C.; and Holmes, B. J.: Flight Evaluation of an Insect Contamination Protection System for Laminar Flow Wings. SAE Paper 850860, April 1985.

[23]Hardy, A. C.; and Milne, P. S.: Studies in the Distribution of Insects by Aerial Currents. Journal of Animal Ecology, vol. 7, 1938, pp. 199-229.

[24]Brooks, T., Pope, D., and Marcolini, M., Airfoil Self-Noise and Prediction, NASA Reference Publication 1218, National Aeronautics and Space Administration, 1989.

[25]Crouch, J.D., Kosorygin, L.L. , Modeling the effects of steps on boundary layer transition, IUTAM Symposium on Laminar-Turbulent Transition, 2006.

[26]Moriarty, P., and Migliore, P., 2003 Semi-empirical aeroacoustic noise prediction code for wind turbines National Renewable Energy Laboratory

[27]Ilinca, F., Hay, A., and Pelletier, D., Shape Sensitivity Analysis of Unsteady Laminar Flow Past a Cylinder in Ground Proximity, Proceedings of the 36th AIAA Fluid Dynamics Conference and Exhibit , AIAA paper 2006 3880, San Francisco, June 2006.

[28]Etienne, S., Hay, A., Garon, A., and Pelletier, D., Shape Sensitivity Analysis of Fluid-Structure Interaction Problems, Proceedings of the 36th AIAA Fluid Dynamics Conference and Exhibit , AIAA paper 2006 3217, San Francisco, June 2006.

[29]Gumber, C. R., Newman, P. A., and Hou, G. J. W., Effect of Random Geometric Uncertainty on the Computational Design of a 3D Flexible Wing, Proceedings of the 20th AIAA Applied Aerodynamics Conference, AIAA paper 2002 2806, St. Louis, June 2002.

[30]Loeven, G.J.A. and Bijl, H., Airfoil Analysis with Uncertain Geometry using the Probabilistic Collocation method, Proc. of the AIAA 48th AIAA/ASME/ASCE/AHS/ASC Structures, Structural Dynamics, and Materials Conference, Schaumburg (IL), United States, 2008.

[31]Iman, R. L. and Conover, W. J. (1980), Small Sample Sensitivity Analysis Techniques for Computer Models, with An Application to Risk Assessment, Communications in Statistics, A9(17), 1749-1842. Rejoinder to Comments, 1863-1874.

[32]Wyss, G.D. and Jorgensen, K.H. (1998) A user's guide to LHS: Sandia's Latin hypercube sampling software. Available online at: http://www.prod.sandia.gov/cgi-bin/techlib/access-control.pl/ 1998/980210.pdf

[33]IEC 61400-1 (1999) Wind turbine generator systems-Part 1: Safety requirements, 2nd edition. International Electrotechnical Commission.

[34]IEC 61400-1 (August 2005) Wind turbines-Part 1: Design requirements, 3rd edition. International Electrotechnical Commission.

[35]Wang, J.F., Periaux, J.,Multi-Point Optimization using GAS and Nash/Stackelberg Games for High Lift Multi-airfoil Design in Aerodynamics, Poceedings of the 2001 Congress on Evolutionary Computation CEC2001 (May 2001), pp. 552-559.

[36]Zhong, B., Qiao, Z., Multiobjective optimization design of transonic airfoils, ICAS-94-2.1.1, 1994.

[37]Tang, Z., Périaux, J., Bugeda,G., Onate, E., Lift maximization with uncertainties for the optimization of high lift devices using Multi-Criterion Evolutionary Algorithms. IEEE Congress on Evolutionary Computation 2009: 2324-2331

[38]Stephens, M.A. 1974. EDF statistics for goodness of fit and some comparisons. Journal of the American Statistical Association 69: 730-737.

[39]Feller, W. 1948. On the Kolmogorov-Smirnov limit theorems for empirical distributions. Annals of Mathematical Statistics 19: 177-189.

[40]Kolmogorov [Kolmogoroff], A. 1941. Confidence limits for an unknown distribution function. Annals of Mathematical Statistics 12: 461-463.

[41]Smirnov [Smirnoff], N. 1939. On the estimation of the discrepancy between empirical curves of distribution for two independent samples. Bulletin de l'Université de Moscou, Série internationale (Mathématiques) 2: (fasc. 2).

[42]Winkler, R.L. 1996. Scoring rules and the evaluation of probabilities. Test 5: 1-60.Yates, F. 1934. Contingency table involving small numbers and the φ^2 test. Journal of the Royal Statistical Society (Supplement) 1: 217-235.

[43]Lindley, D.V., A. Tversky and R.V. Brown. 1979. On the reconciliation of probability assessments. Journal of the Royal Statistical Society A 142 (Part 2): 146-180.

[44]de Finetti, B. 1962. Does it make sense to speak of good probability appraisers? Pages 357-363 in The Scientist Speculates: An Anthology of Partly-Baked Ideas, I.J. Good (ed.). Wiley, New York.

[45]Brier, G.W. 1950. Verification of forecasts expressed in terms of probability. Monthly Weather Review 78: 1-3.

[46]Song, K.-S.. 2002. Goodness-of-fit tests based on Kullback-Leibler discrimination information. IEEE Transactions on Information Theory 48:1103-1117

[47]Kullback, S. 1959. Information Theory and Statistics. Wiley, New York.

[48]Kullback, S., and R.A. Leibler. 1951. On information and sufficiency. Annals of Mathematical Statistics 22: 79-86.

[49]Mathiassen, J.R., A. Skavhaug and K. Bø. 2002. Texture similarity measure using Kullback-Leibler divergence between gamma distributions. Pages 19-49 in Computer Vision - ECCV 2002: 7th European Conference on Computer Vision, Copenhagen, Denmark, May 28-31, 2002. Proceedings, Part III. Lecture Notes in Computer Science, volume 2352. Springer, Berlin.

[50]Kalyanmoy Deb, Amrit Pratap, Sameer Agarwal, and T. Meyarivan. A Fast Elitist Multi-objective Genetic Algorithm: NSGA-II. IEEE Transactions on Evolutionary Computation, 6(2):182-197, April 2002

[51]Oberkampf, W.L., and M.F. Barone. 2006. Measures of agreement between computation and experiment: validation metrics. Journal of Computational Physics 217: 5-36.

[52]Justesen, P., Ursem, R., Many-objective Distinct Candidates Optimization using Differential Evolution on centrifugal pump design problems. Proceedings of the IEEE Congress on Evolutionary Computation, CEC 2010, Barcelona, Spain, 18-23 July 2010